CHAPTER 5

RESULTS AND DISCUSSIONS

In this chapter, the results on characterization of ZnO(Al) thin films fabricated in this thesis are discussed. First, the influence of the RF power and the argon gas pressure on the deposition rates in each target will be described. Next, the results of the characterization of ZnO(Al) thin films such as the structural properties, the electrical properties, the optical properties and the figure of merit will be shown.

5.1 Deposition Rates of ZnO(Al) Thin Films

In this work, we calculated the films thickness from transmission spectra as described in Chapter 4 by using Eq. 4.3. All films were deposited at the same thickness of about 500 nm in each sputtering condition. The deposition time was in the range of 60–140 mins depending on the sputtering conditions. For example, the deposited films of the same target with increasing RF power from 50 W to 125 W, the deposition time decreases from 140 mins. to 60 mins., respectively. The deposition rate is the ratio of the films thickness to the deposition time. Figure 5.1 shows the deposition rate of the films from each target as a function of the argon gas pressure. For the planar sputtering, the deposited films were not uniform on the substrate, so these deposition rates were the average value over the area of the films. As shown in Fig. 5.1, we found that the deposition rates differed insignificantly. At the same argon gas pressure, the deposition rates from each target were less than 1 nm/min difference and independent with the Zn content added in the target. However, the influence of the argon gas pressure on the deposition rate of each target shows the same trend, that is the deposition rates gradually decrease as the argon gas pressure increases. This is probably because at higher argon gas pressure, the mean free path of the sputtered atoms decreases, resulting in many collisions of atoms and leading to the scattering of sputtered atoms and decreasing of kinetic energy.

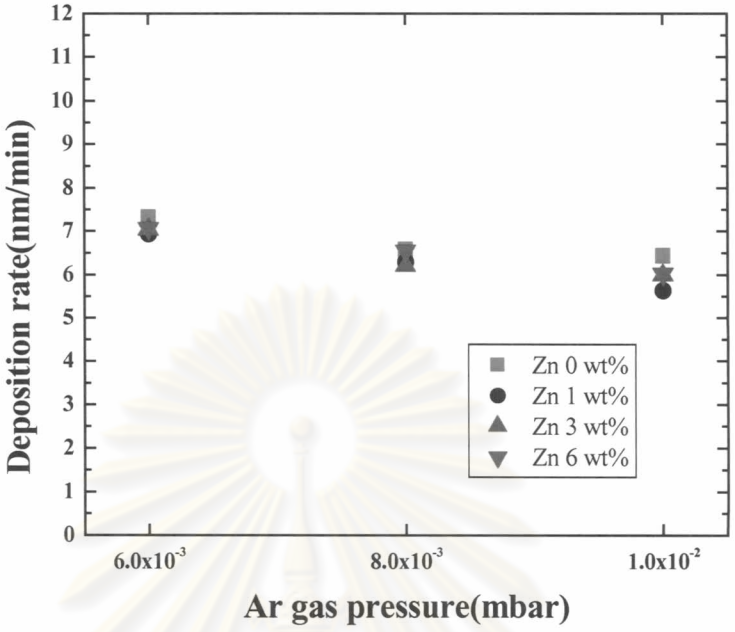

Figure 5.1: Deposition rates of the films in each target as a function of the argon gas pressure at the RF power of 100 W.

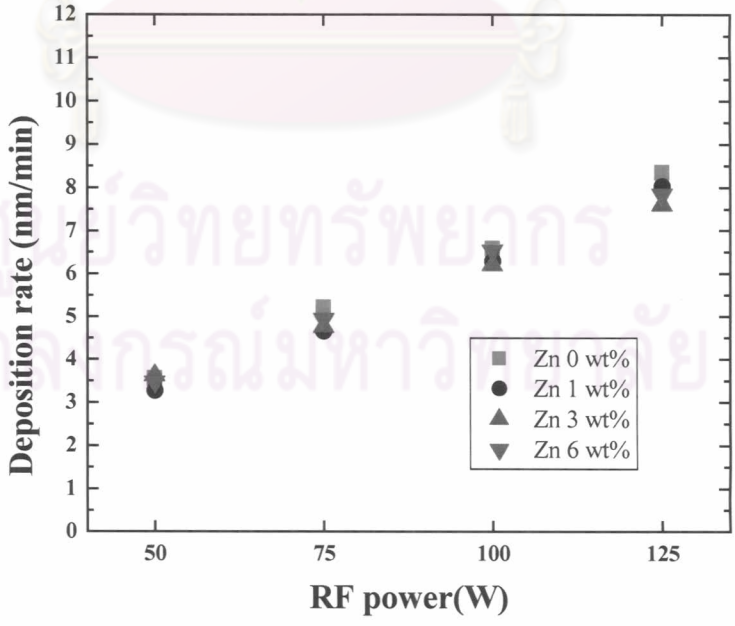

Figure 5.2: Deposition rates of the films in each target as a function of the RF power at the argon gas pressure of 8.0×10^{-3} mbar.

Considering the influence of the RF power on the deposition rates, we found that the deposition rate was linearly increased with the increasing RF power as shown in Fig. 5.2. At the RF power of 125 W, the deposition rates are about 2.5 times higher than that of 50 W. Higher RF power means higher current and higher voltage. Therefore, the number of argon ions increases and have higher energy. Thus the number of sputtered atoms at the target surface increases due to the enhancement of the bombardment by argon ions as the RF power increases resulting in the increase of the deposition rate. We found that the deposition rate as varying the RF power was more significant than those with varying argon gas pressure. From these results, the deposition rate is inversely proportional to the argon gas pressure and proportional to the RF power.

5.2 Structural Properties

To check all possible peaks of intensity that were detected from the ZnO(Al) thin films, the XRD system was set to perform a rough scan with a step scan of 0.1° and a step time of 0.6 s. Figure 5.3 (a) shows XRD patterns of the ZnO(Al) thin films deposited at different argon gas pressures. The XRD measurements were taken on the central region of the samples. Note that all XRD peaks in Fig. 5.3 (a) came from the films having about the same thickness (~500 nm). At the same Zn content, all films show only the (002) peak in the displayed–2θ region at $2\theta \approx 34.2^{\circ}$ and no peaks of metallic Zn or Al. This indicates that the ZnO(Al) films fabricated by the RF magnetron sputtering were polycrystalline with a hexagonal structure and a preferred orientation with c–axis perpendicular to the substrate [13,14,19]. These peaks showed a deviation from 34.44° which is the value of standard ZnO powder (JCPDS 05–0664) but they agree well with the value reported in the literature for the ZnO(Al) thin films [13,14]. The impact of argon gas pressure on intensity of (002) peak is small in argon gas pressure from 6.0×10^{-3} to 1.0×10^{-2} mbar due to insignificantly varying argon gas pressure, i.e. the intensity of (002) peak is slightly decreased when decreasing the argon gas pressure.

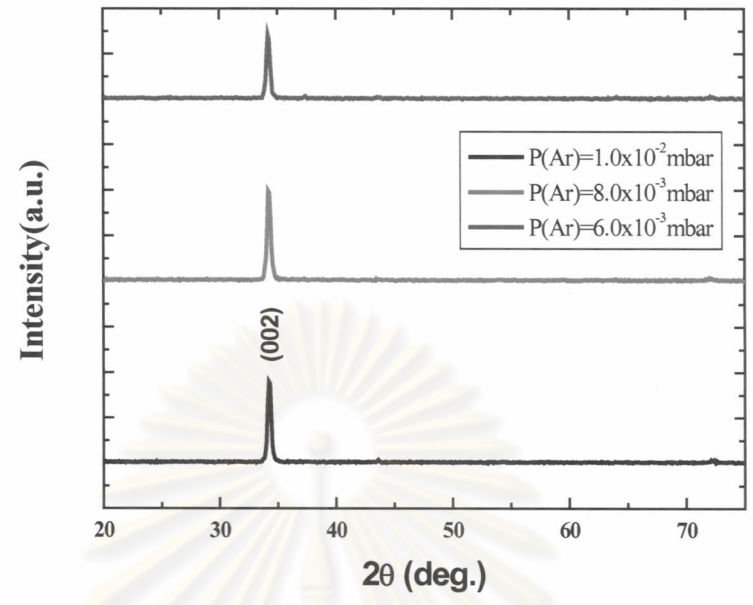

(a)

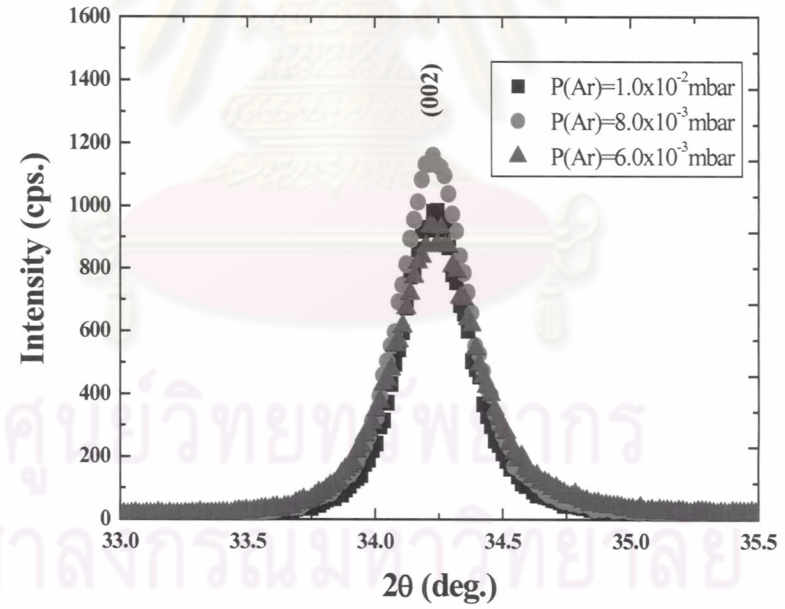

(b)

Figure 5.3: The X–ray diffraction (XRD) patterns of the ZnO(Al) films deposited at different argon gas pressures for the RF power of 100 W, (a) a rough scan with a step scan of 0.1° and a step time of 0.6 s, (b) a fine scan with a step scan of 0.015° and a step time of 3 s.

For fine scan, the XRD system was set to the range of 2θ which scanned only the peaks in displayed–2θ regions detected from Fig. 5.3 (a). The system was set with a step scan of 0.015° and a step time of 3 s for fine scan. The peak from the fine scan was used to calculate the grain size of the films using the *FWHM*. Figure 5.3 (b) shows fine scan XRD patterns of the ZnO(Al) thin films deposited at different argon gas pressures. We calculated the *FWHM* from the peak of fine scan as shown in Fig 5.3 (b). Moreover, we calculated the grain size of the films from the *FWHM* as a function of argon gas pressure as shown in Fig. 5.4. The change in *FWHM* generally reflects the change in the grain size of the crystallites, i.e. the increase in *FWHM* corresponds to the decrease in grain size. The data show that the trend of grain size of the films gradually increases with increasing argon gas pressure. This can be explained by; at lower argon gas pressure, the mean free path of the sputtered atoms increases, resulting in less collision of atoms and leading to the increasing of energetic ion bombardment on the grain surfaces, thus making them smaller. Also the crystallinity of the films is deteriorated, so the grain becomes smaller.

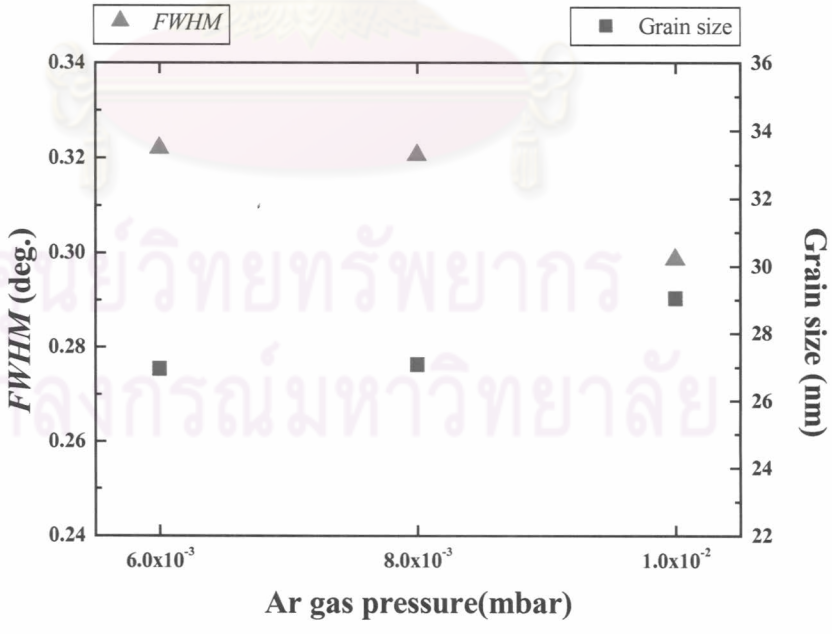

Figure 5.4: Full width at half maximum (FWHM) of XRD (002) peaks and the grain size for ZnO(Al) films deposited at various argon gas pressures for the RF power of 100 W.

The XRD patterns of the ZnO(Al) thin films deposited at different RF powers are shown in Fig. 5.5. We note that all the films compared here have about the same thickness (~500 nm). It was found that the intensity of (002) peak decreases with increasing RF power. The films deposited at the RF power of 50 W show a (002) peak with relatively highest intensity. This shows that the crystallinity of the films prepared at 50 W is better than that of the others, resulting in the narrower and sharper intensity of the diffraction peak. As suggested by Ondo–Ndong et al. [19], this can be explained by the nucleation kinetics and the films growth that are influenced by the interactions between the substrate and the incoming energetic atoms on the film crystallinity. The formation of adatoms on the substrate is at the suitable condition according with deposition rate and kinetic energy of the adatoms. However at higher power, the (002) peak intensity decreases indicating the crystallinity deterioration of the films due to higher energy of ion bombardment. Furthermore, the formation time of adatoms used to reorganize themselves on the substrate is not sufficient due to high deposition rate. This results in the creation of more defects such as Zn interstitial atoms and oxygen vacancies. Moreover, the substrate temperature was set at room temperature, thus the formation energy from substrate was not sufficient to promote the diffusion length of the adatoms.

The grain size and the *FWHM* of the films at varying the RF powers were calculated from Fig. 5.5 (b) and shown in Fig. 5.6. The *FWHM* increases with the increase of the RF powers from 50 W to 125 W. This is because the energetic ion bombardment on the grain surfaces can lead to deterioration, so the grains become smaller and the columnar growth is interrupted. Furthermore, at higher RF power, the formation time of adatoms on the substrate is not sufficient due to high deposition rate, thus many small grains were generated.

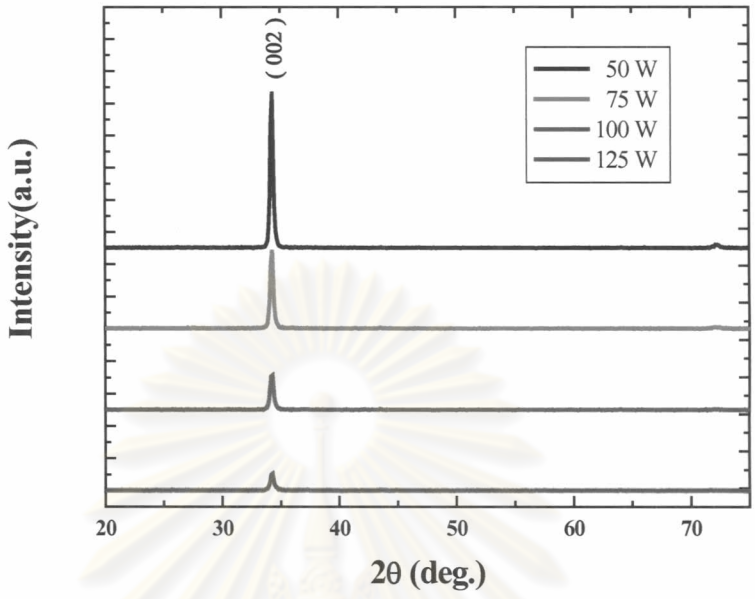

(a)

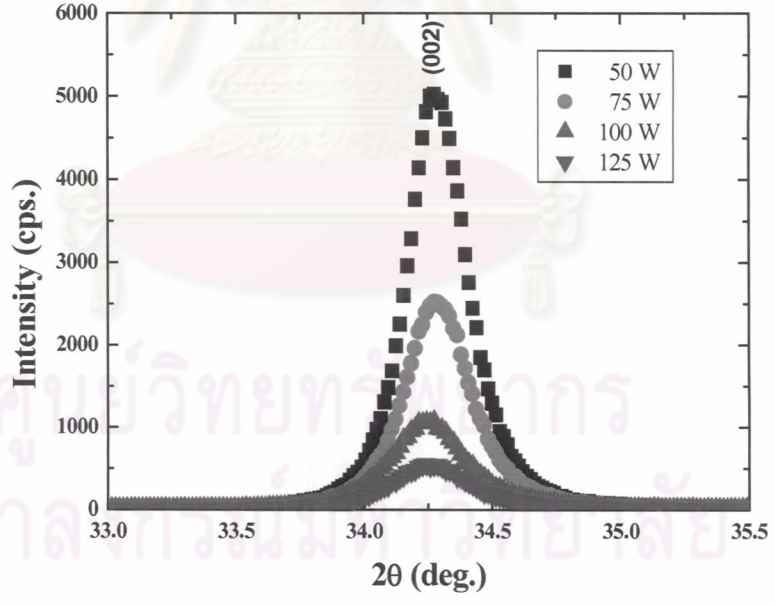

(b)

Figure 5.5: The X–ray diffraction (XRD) patterns of the ZnO(Al) films deposited at different RF powers for the argon gas pressure of 8.0×10^{-3} mbar, (a) a rough scan with a step scan of 0.1° and a step time of 0.6 s, (b) a fine scan with a step scan of 0.015° and a step time of 3 s.

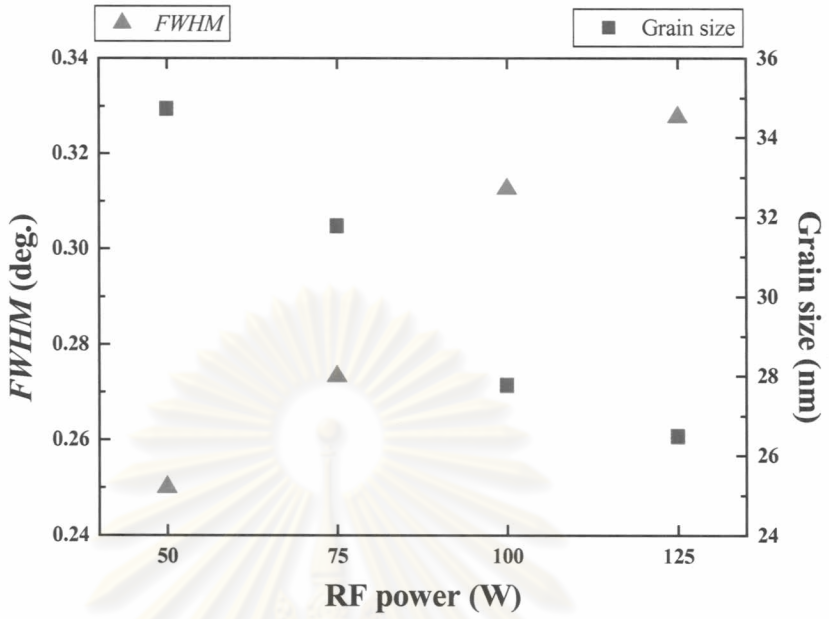

Figure 5.6: Full width at half maximum (FWHM) of XRD (002) peaks and the grain size of the ZnO(Al) films deposited at various RF powers for the argon gas pressure of 8.0×10^{-3} *mbar.*

The XRD patterns of the ZnO(Al) thin films deposited from different targets are shown in Fig. 5.7. Similarly, the films show only the (002) peak in the displayed–2θ region at $2\theta \approx 34.2^{\circ}$. The film deposited from ZnO(Al) target without Zn content (0 wt%) shows a (002) peak with relatively highest intensity, while the films deposited from the ZnO(Al) targets with Zn content of 1 wt% , 3wt% and 6 wt% show the (002) peaks with lower intensity indicating that the Zn content influences the crystallinity of the films.

The grain sizes of the films as a function of Zn content (wt%) were calculated and shown in Fig. 5.8. The *FWHM* is increased when the Zn content is increased from 0 wt% to 6 wt%. As a consequence, the grain size decreases as the Zn content increases. The grain size becomes smaller with the increasing Zn content due to more Zn interstitial atoms in the films acting as impurities. They may cause the interruption of the columnar growth, thus the grain size becomes smaller.

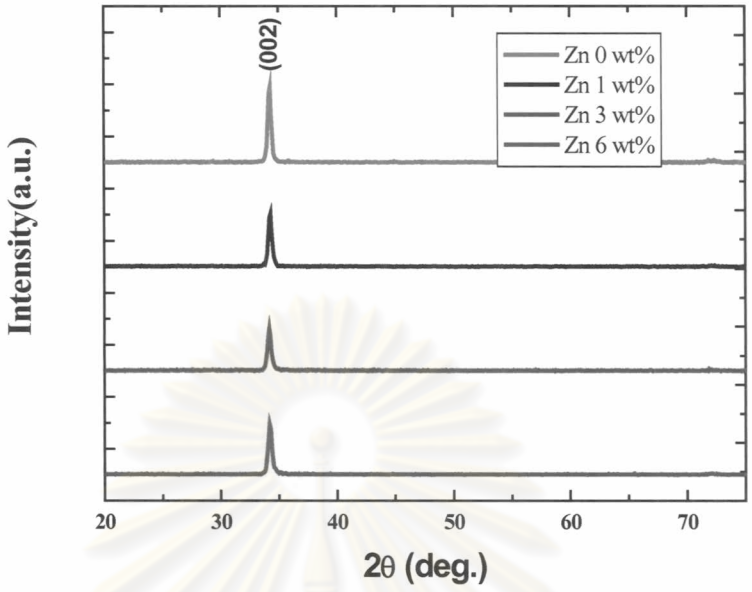

(a)

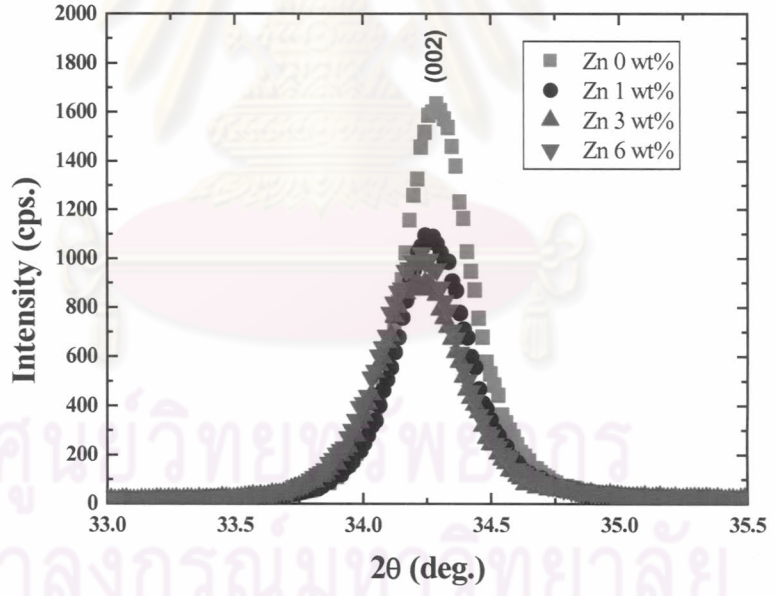

(b)

Figure 5.7: The X–ray diffraction (XRD) patterns of the ZnO(Al) films deposited from different targets for the argon gas pressure of 8.0 $\times 10^{-3}$ mbar and the RF power of 100 W, (a) a rough scan with a step scan of 0.1° and a step time of 0.6 s, (b) a fine scan with a step scan of 0.015° and a step time of 3 s.

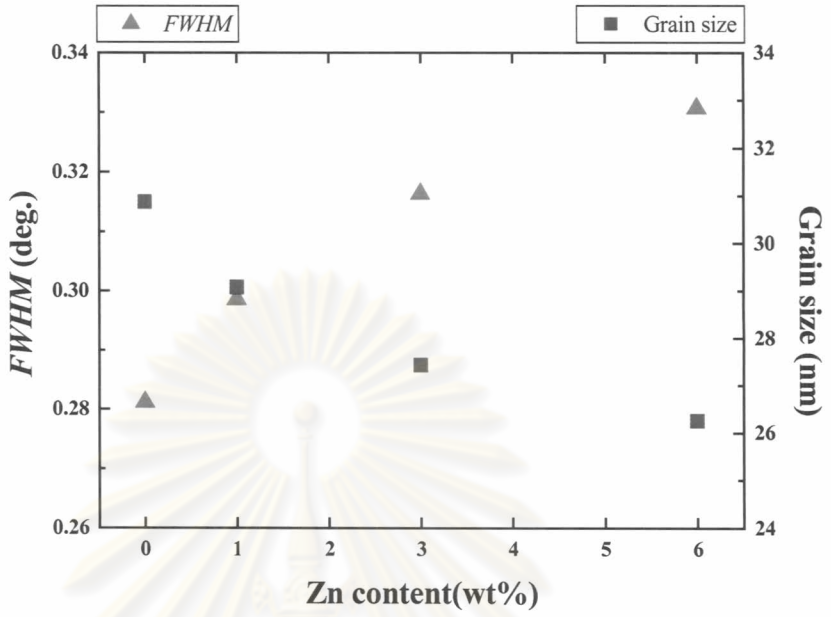

Figure 5.8: Full width at half maximum (FWHM) of XRD (002) peaks and the grain size of ZnO(Al) films deposited from different targets for the argon gas pressure of 8.0×10^{-3} *mbar and the RF power of 100 W.*

5.3 Electrical Properties

For planar sputtering, the substrates are rotated in circle parallel and off–axis to the surface of the target during the deposition, as shown in Fig. 5.9 (a). The films obtained from the deposition are not thoroughly uniform on the 4.85 cm × 5.85 cm SLG substrates. The substrate is divided into three zones; Zone A, Zone B and Zone C, where Zone A is closest to the center of rotation. All films have the symmetry as shown in Fig. 5.9 (b).

The Hall measurement shows that all ZnO(Al) films are degenerate doped n–type semiconductor. The resistivity of the films as a function of the RF power from two different targets (0 wt% and 6 wt%) is shown in Fig. 5.10 (a). All of the films were deposited at the same argon gas pressure of 8.0×10^{-3} mbar and the substrate temperature was initially set at room temperature. The resistivity in the same zone of the films from different targets with varying the RF power was compared. It was

found that, at the Zn content of 0 wt%, the resistivity in each zone decreases with increasing RF power from 50 W to 125 W. For the Zn content of 6 wt%, the resistivity in each zone decreases with increasing RF power from 50 W to 100 W and slightly increases when the RF power reach 125 W.

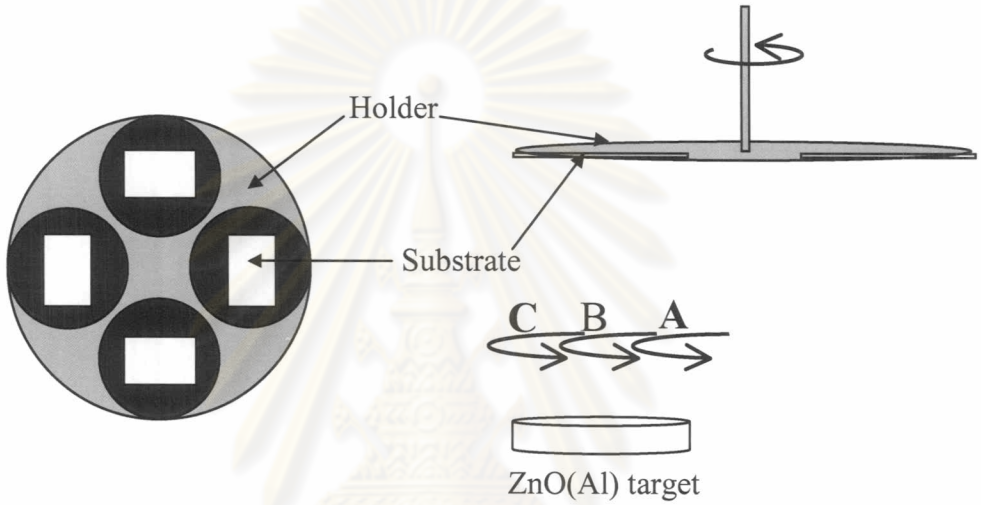

(a)

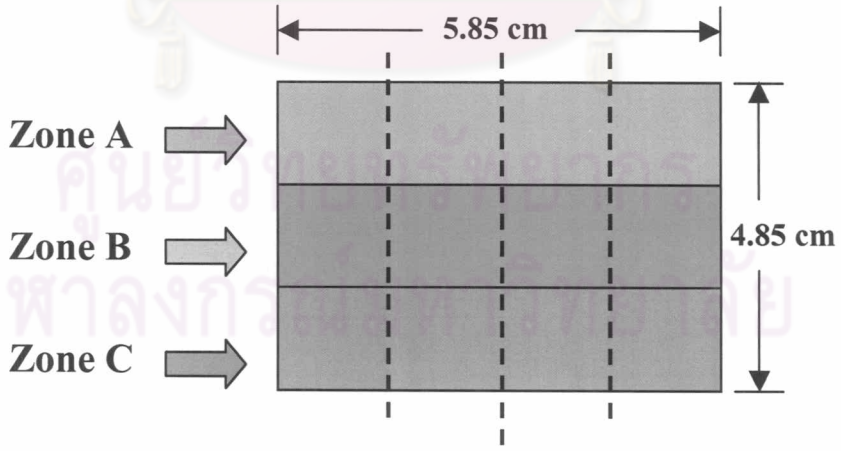

(b)

Figure 5.9: (a) Configuration of planar sputtering, (b) Three zones of the films on the SLG substrate.

The lowest resistivity of the order of 10^{-3} Ω·cm was achieved at the Zn content of 0 wt% and RF power of 125 W. As shown in Chapter 3, the resistivity is proportional to the inverse product of the carrier concentration and the Hall mobility. Therefore, the change in the resistivity with the RF power as shown in Fig. 5.10 (a), is ascribed to the change in carrier concentration and/or Hall mobility which are characteristic parameters reflecting the films properties and/or the impurity content of the films. It can be explained that the number of intrinsic donors (oxygen vacancies and Zn interstitial atoms) increases due to the decrement of formation time of the adatoms on the substrate as the RF power increases. The surface diffusion and re–organization of the adatoms is limited. Thus, small grains and defects like oxygen vacancies and Zn interstitial atoms are formed. The conduction mechanism is governed by a high concentration of donor type intrinsic defects, which results in low resistivity. This agrees with the structural properties shown in Fig. 5.5 (see section 5.2 for structural properties and further discussion).

In general, for the aluminum doped zinc oxide, an aluminum atom is considered to substitute for a zinc atom and acts as a donor. Therefore, the increment of carrier concentration, when the RF power increases as shown in Fig. 5.10 (b), can be assumed. At low RF power, only little energy is transferred to the target by argon ions. The energy of argon ions is not enough for a complete dissociation of Al_2O_3 molecules. At high RF power, higher energies of argon ions provide enough energy for a complete dissociation of Al_2O_3 molecules. So, the number of aluminum atoms in the films increases, resulting in the increasing of the carrier concentration (see Fig. 5.10 (b)). Also this assumption supports to the change in the resistivity and the carrier concentration of the films [35].

For the Zn content of 6 wt%, the Hall mobility of the films increases with the increase of RF power from 50 W to 100 W and slightly drops at the RF power of 125 W. Generally, the increasing of grain boundary cause the decreasing in Hall mobility. But our work shows that the enhancement of the grain boundary (this is due to the films have smaller grain size (see Fig. 5.6)) does not influence on the Hall mobility from RF power 50 W to 100 W because the Hall mobility is still high. But at RF power of 125 W, the grain boundary start to have the influence on the Hall mobility due to the decrease of Hall mobility.

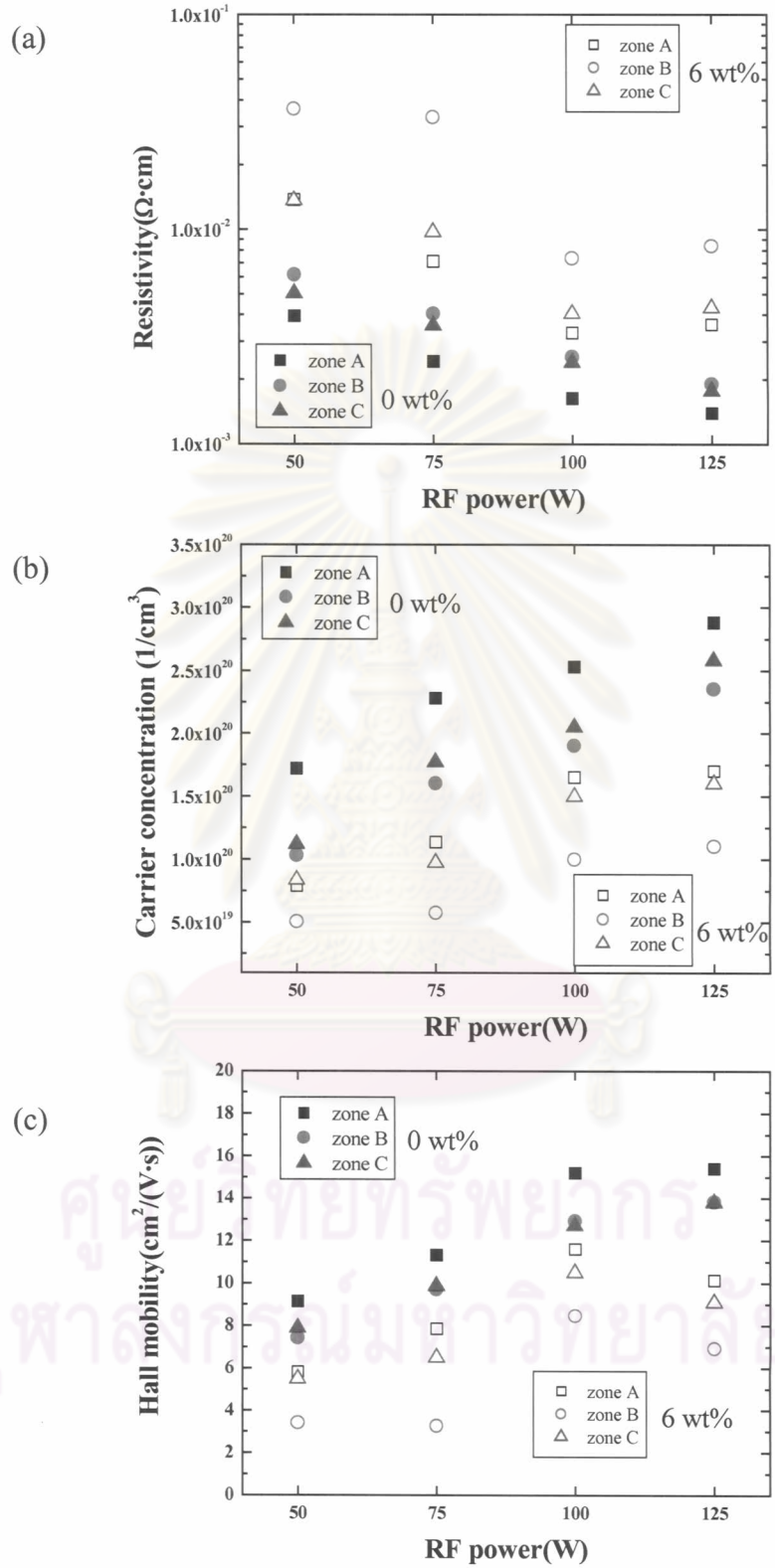

Figure 5.10: Dependence of resistivity (a), carrier concentration (b), and Hall mobility (c) of ZnO(Al) thin films on the RF power at argon gas pressure of 8.0 × 10^{-3} mbar.

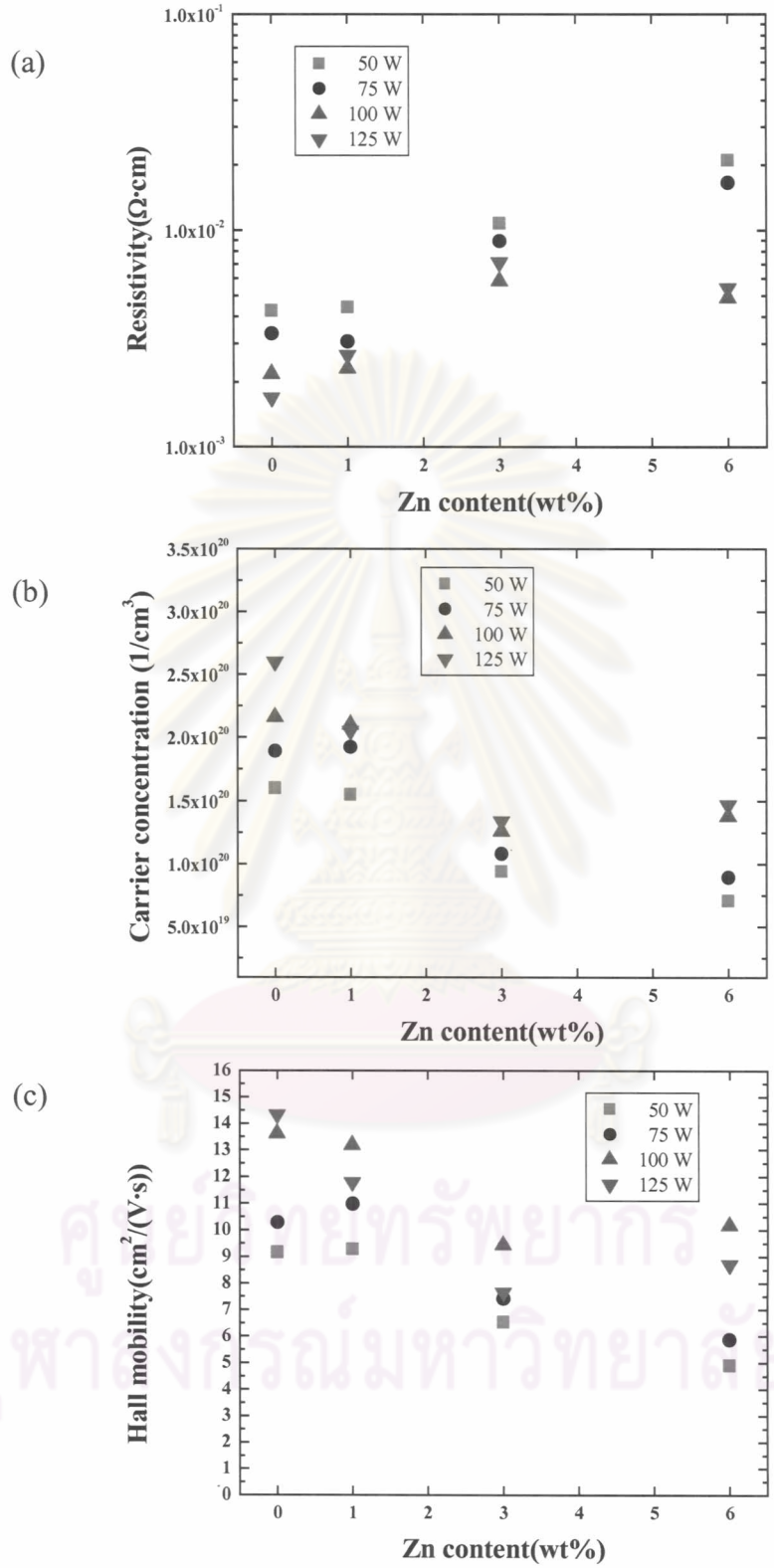

Figure 5.11: Dependence of resistivity (a), carrier concentration (b), and Hall mobility (c) of ZnO(Al) thin films on Zn content. The films were deposited at various RF powers and the argon gas pressure of 8.0 × 10^{-3} mbar.

Apart from this, the crystallinity of the films, which is deteriorated due to bombardment of high energy, can also decrease the Hall mobility because of the limitation of the carrier path. For this reason, the resistivity slightly increased when the RF power of 125 W due to decreasing in the Hall mobility of the films.

Since the electrical properties of the films in each zone showed the same trend, so we will use the average values of these data (resistivity, carrier concentration and the Hall mobility) over the whole substrate (Zone A, B and C). Figure 5.11 (a), (b), and (c) show the resistivity, the carrier concentration and the Hall mobility, respectively, as a function of the Zn content (wt%). The films were deposited at RF power of 50 W to 125 W and the argon gas pressure of 8.0×10^{-3} mbar. The influence of RF power on the resistivity, the carrier concentration and the Hall mobility with varying Zn content shows 2 different types of variation due to low RF power (50 W and 75 W) or high RF power (100 W and 125 W).

At low RF power, the resistivity of the films increased with increasing Zn compositions. This can be explained using the proposed model as shown in Fig. 5.12.

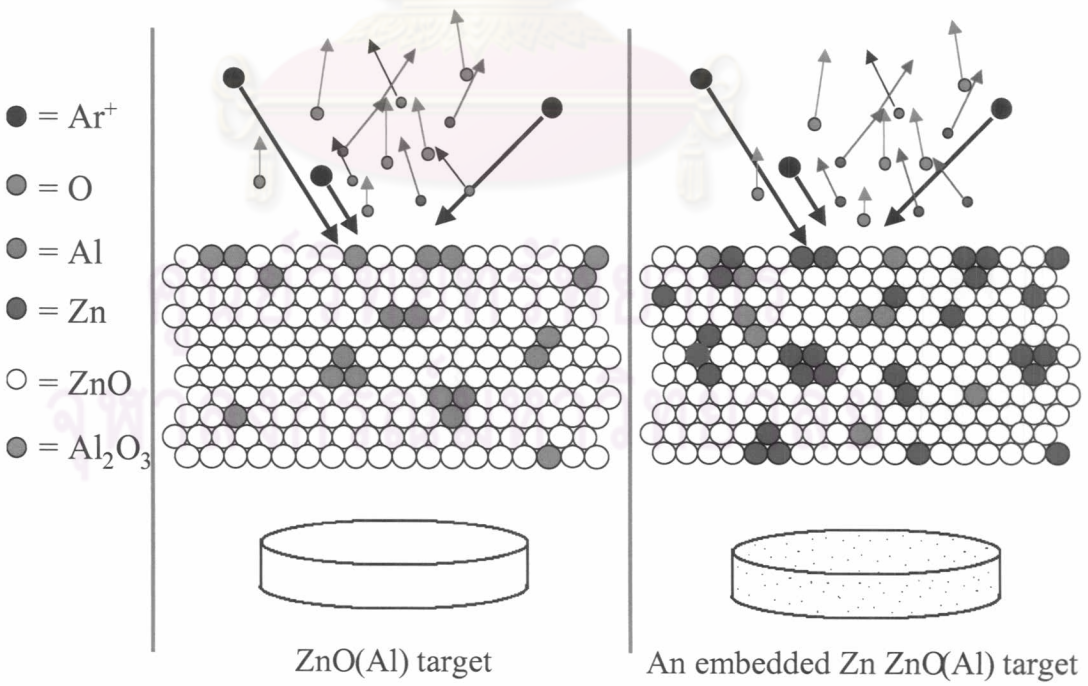

Figure 5.12: A model showing a cross section of ZnO(Al) target and an embedded–Zn ZnO(Al) target.

The addition of Zn to the target causes the metallic Zn to spread out in the target. Thus, the probability of the Zn atoms being sputtered increases, resulting in the decreasing of sputtered Al_2O_3 molecules. Consequently, there are less number of Al atoms at the lattice sites in the ZnO(Al) films, and the carrier concentration decreases. We recall that the carriers due to the contribution from Al atoms on the substitution sites of Zn atom yield better electrical conductivity in the ZnO(Al) films than that from the oxygen vacancies and the Zn interstitial atoms. From this reason, the resistivity of the films increases when increasing Zn content in target. For the reason of the decrease of the Hall mobility, we propose that there are more Zn interstitial atoms obstructing the carriers, which act as the scattering centers.

At high RF power, it was found that the resistivity of the films increased when the added Zn compositions were changed from 0 wt% to 3 wt%. This can be explained by the same reason as described above. But for the Zn content of 6 wt %, it turned out that the resistivity dropped, and could be used as the critical value of the Zn content for the RF power of 100 W and 125 W. The drop of resistivity was achieved by the excess Zn metal in the films resulting in increasing of the Zn interstitial atoms being consistent with higher of carrier concentration (see Fig 5.11(b)).

For the lower value of Hall mobility at Zn content of 0 wt% to 3wt%, we similarly propose that there are more Zn interstitial atoms obstructing the carriers, which act as the scatterers. From Figs. 5.7 and 5.8, the Zn contents show an influence on the crystallinity of the films. Higher Zn content yields smaller grain size. The films have smallest grain size with the Zn content of 6 wt%. In Fig. 5.11 (b) showing the films with high carrier concentration ($\approx 10^{20}$ cm^{-3}), the carriers can probably tunnel through the grain boundary [36], resulting in the increasing of the Hall mobility. Thus this promotes the decreasing of the resistivity of the films.

5.4 Optical Properties

The transmission spectra of the ZnO(Al) films fabricated from ZnO(Al) target with Zn 6 wt% at different RF powers are shown in Fig. 5.13. These transmission (%T) values were measured in the central region of Zone B of the films at the argon gas pressure of 8.0×10^{-3} mbar and the RF power of 50, 75, 100 and 125 W. All samples are comparatively at the same thickness. The impact of the RF power on the transmission is very small for the RF power between 50 W and 100 W. The average transmission of above 90% was obtained in the wavelength range of 400 to 1000 nm, showing the excellent transparency of the films. But for the RF power of 125 W, the average transmission drops to about 80% in the same range of wavelengths. Moreover, the deposited films show the metal–like thin films with brown coloration formed by excess defects (especially Zn metal), thus decreasing the transmission of films. This can be said that the films have poor transparency. We recall that the ZnO(Al) thin films have poor crystallinity due to high RF power (see Fig. 5.5), so that the defects such as Zn interstitial atoms, oxygen vacancies and Al on the Zn site increased. Therefore, the carrier concentration increased with increasing RF power (see Fig 5.10 (b)). This decrease in the transmission at long wavelength is attributed to the increase of free carrier absorption. The absorption edge of the transmission shifted to the shorter wavelength (blue shift) with increasing RF power. This effect is attributed to the Burstein–Moss effect, since the absorption edge of a degenerate semiconductor is shifted to the shorter wavelength with increasing free carrier concentration [14].

Figure 5.14 shows the transmission spectra of the films fabricated from different targets at fixed argon gas pressure of 8.0×10^{-3} mbar and RF power of 100 W. The Zn content has the following impacts on the transmission:

- For the wavelength below 1000 nm, the impact of the Zn content is very small. All the films have the average transparency of over 90%. The transparency of the films is excellence in the range of visible light.

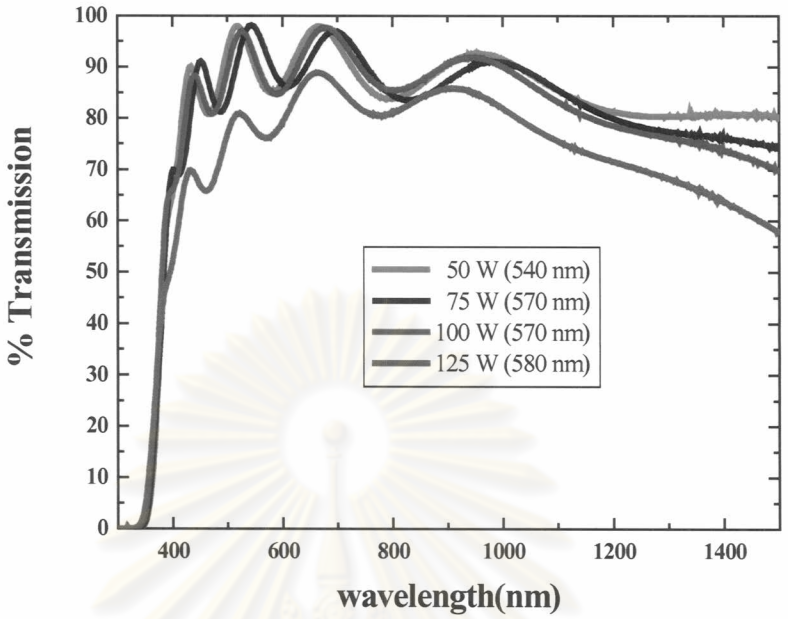

Figure 5.13: Transmission spectra of the films as a function of RF power at the argon gas pressure of 8.0×10^{-3} mbar.

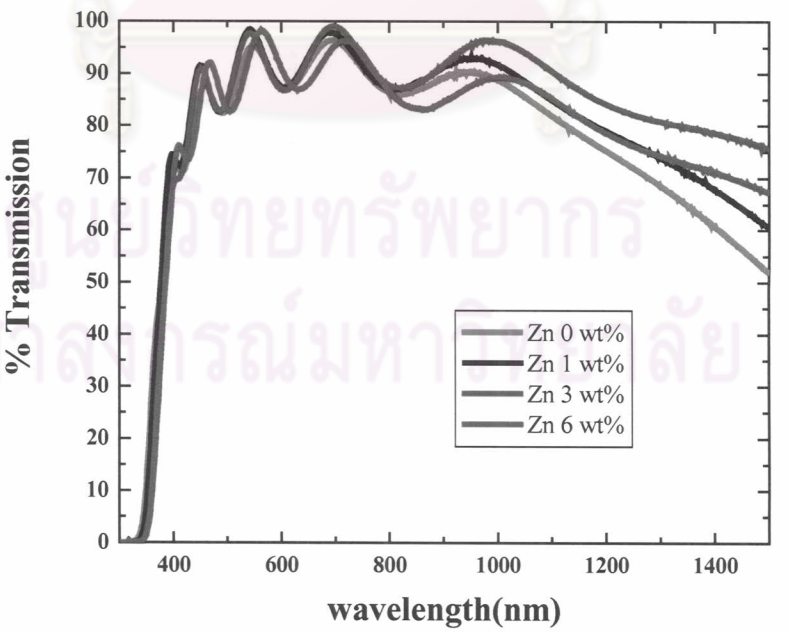

Figure 5.14: Transmission spectra of the films as a function of Zn content (wt%) at the argon gas pressure of 8.0×10^{-3} mbar and the RF power of 100 W.

- For the wavelength above 1000 nm, the transmission of the films increases when the Zn content are changed from 0 wt% to 3 wt% and decreases at the Zn content of 6 wt%.

The increase of transmission with increasing Zn content from 0 wt% to 3 wt% at the RF power of 100 W corresponds to the decrease of carrier concentration shown in Fig. 5.11 (b). In addition the decrease of free carrier absorption results in the increase of the transmission in the infrared region. However, as the Zn content increasing to 6 wt%, the transmission of the deposited thin films significantly decreases especially in the infrared region, being consistent with increasing of the carrier concentration (see Fig. 5.11 (b)).

For the films fabricated with Zn content of 0 wt% to 3 wt% the absorption edges of the transmission shift to the longer wavelength (red shift). These results are consistent with the decrease of carrier concentration in Fig. 5.11 (b). However, for the Zn content of 6 wt%, the absorption edge shifts back to the shorter wavelength (blue shift). This blue shift is ascribed to the increase of carrier concentration due to the high content of Zn atoms.

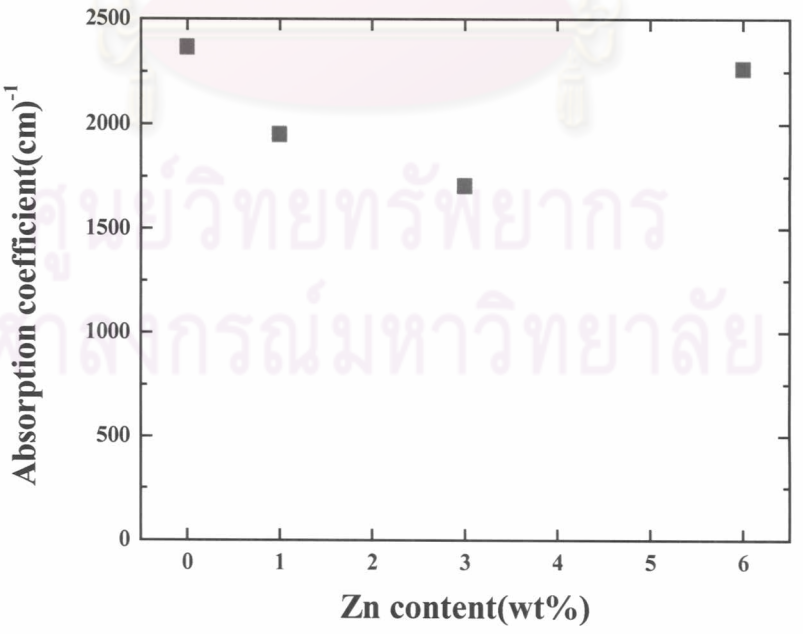

Figure 5.15: Averaged values of absorption coefficient of the films as a function of Zn content at the argon gas pressure of 8.0 $\times 10^{-3}$ mbar and the RF power of 100 W.

Figure 5.15 shows averaged values of the absorption coefficient in the wavelength region 400–1200 nm as a function of Zn content in the targets. For the Zn content of 0 wt%, the film exhibits the highest absorption coefficient of about 2300 cm^{-1}. This is because the 0 wt% Zn films show a relatively low transmission in this region of wavelengths. At the Zn content of 3 wt% the film has the lowest absorption coefficient of about 1700 cm^{-1} because it has relatively high transmission. Figure 5.11 (a) shows that the resistivity of the film for RF power of 100 W increases when the added Zn compositions are changed from 0 wt% to 3 wt%, and it decreases when the Zn content is increased to 6 wt% in the target. This trend is better for achieving the conductivity again, but the trend of the absorption coefficient of films would be increased as shown in Fig. 5.15. This means that it is not necessary to increase the Zn content to more than 6 wt% because the transmission of the films would be diminished.

Because the ZnO(Al) thin film has a direct gap semiconductor, the optical energy gap of the film can be obtained by plotting $(\alpha h\upsilon)^2$ vs. $h\upsilon$, where α is absorption coefficient and $h\upsilon$ is photon energy. The photon energy at the point where $(\alpha h\upsilon)^2$ is zero is E_g [13]. Figure 5.16 shows the variation of optical energy gap as a function of RF power using the target with Zn content of 6 wt%. The extrapolation of the linear segments of the curves towards the x–axis gives the E_g values in the range 3.46–3.57 eV, whereby the smallest and the largest energy gap correspond to the highest and lowest resistivity of the films, respectively, as shown in Fig. 5.10 (a). The higher E_g has been attributed to the Burstein–Moss effect caused by an increase of free carrier concentration as shown in Fig.5.10 (b). Since the free carrier concentration increases, the electrons would fill all states of valence band and partially some states of conduction band. Therefore, for the transition of electrons from the filled valence band to the unoccupied conduction band, they require higher energy than energy level of the occupied state in conduction band, resulting in the widening energy gap of the films.

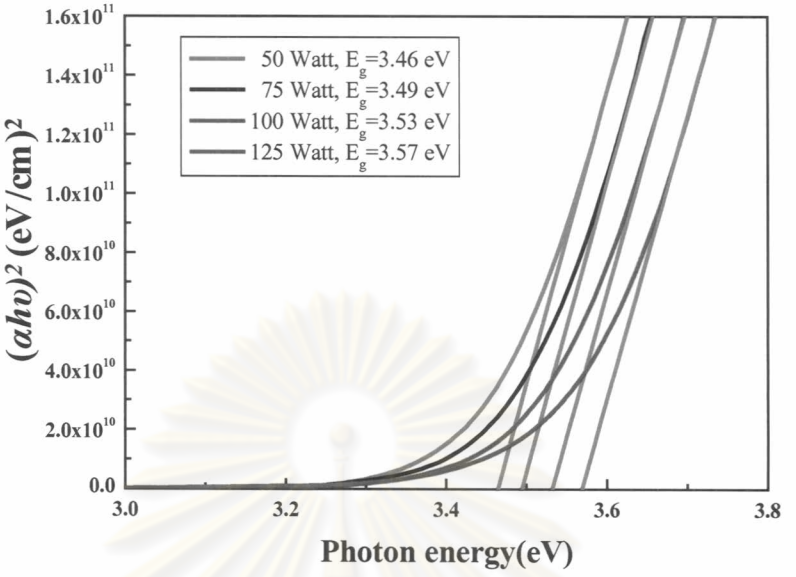

Figure 5.16: Plots of $(\alpha h\upsilon)^2$ versus $h\upsilon$ for ZnO(Al) films grown at the argon gas pressure of 8.0 $\times 10^{-3}$ mbar, and various RF powers using the target with Zn content of 6 wt% .

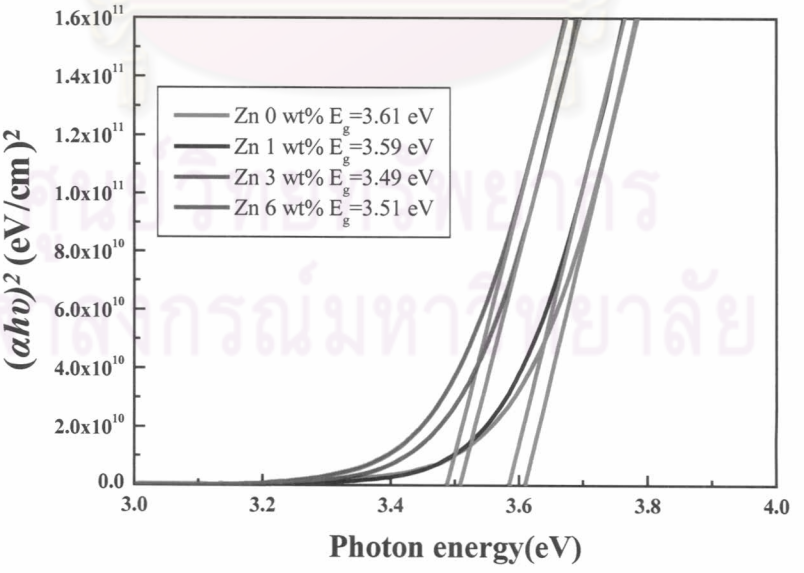

Figure 5.17: Plot of $(\alpha h\upsilon)^2$ versus $h\upsilon$ for ZnO(Al) films grown at the argon gas pressure of 8.0$\times 10^{-3}$ mbar, the RF power of 100 W and various the Zn contents.

Figure 5.17 shows the variation of the optical energy gap as a function of the Zn content. It shows that the energy gap narrows (red shift) with increasing Zn content from 0 wt% to 3 wt%. This narrowing effect can be understood based on the Burstein–Moss effect. For the Zn content 6 wt% showed the energy gap slightly increases again (blue shift). This broadening effect is pointed out that there is an increase in Fermi level due to the increasing free carrier concentration [13].

5.5 Figure of Merit

For application of the ZnO(Al) thin films as a window layer for $Cu(In,Ga)Se_2$ thin films solar cells, the ZnO(Al) films must have a high average transmission in the wavelength less than 1200 nm (correspond with photon energy greater than the energy gap of $Cu(In,Ga)Se_2$ solar cells and can create electron–hole pairs). Moreover, the ZnO(Al) thin films must have a low resistivity. The dependency and complexity can be lifted by considering a figure of merit (*FOM*) is defined as [37]

$$FOM \equiv \frac{-1}{\rho \ln(T)}, \tag{5.1}$$

where ρ is the electrical resistivity and T is the transmission.

Figure 5.18 shows *FOM* of the ZnO(Al) films from different targets deposited at argon gas pressure of 8.0×10^{-3} mbar and RF power of 100 W. The higher *FOM* means good films properties, i.e. high optical transparency and low resistivity. The films from Zn content of 1 wt% show the highest *FOM* of about 3700 $(\Omega\cdot cm)^{-1}$ due to its low resistivity (see Fig. 5.11 (a)), although it does not have the highest transmission (averaged in the 400–1200 nm wavelength (see Fig. 5.14)). However, its transmission is still high enough. For the films prepared from the ZnO(Al) target with no Zn content added (0wt%), although it does have the lowest resistivity (see Fig. 5.11 (a)) but it does not show the highest *FOM* due to its lowest transmission (averaged in the 400–1200 nm wavelength (see Fig. 5.14)). While for the Zn content of 3 wt%, it has the highest transmission (averaged in the 400–1200 nm wavelength (see Fig. 5.14)) but the *FOM* yields relatively low value due to its highest resistivity (see Figs. 5.11 (a)).

Lee et al. [37] investigated the optoelectronic properties and the *FOM* of the ZnO(Al) thin films using the ZnO(Al) (Al_2O_3 2.5 wt%) under various argon gas pressures between 2–30 mTorr (~2.67×10^{-3}–4.0×10^{-2} mbar). Other deposition conditions were kept constant to be RF power of 120 W and no intentional substrate heating. They found that the ZnO(Al) films deposited at 2 mTorr (~2.67×10^{-3} mbar) showed lowest resistivity of about 1×10^{-3} Ω·cm, while the transmission was less affected by the pressure and still above 85% (averaged in the 400–800 nm wavelength region) in whole investigated pressure range. Moreover, the 2 mTorr film showed highest *FOM* of about 6000 $(\Omega\cdot cm)^{-1}$. But, if we calculated the *FOM* of our samples from the average value of the transmission in the 400–800 nm wavelength region then the film for Zn content of 1 wt% still shows the highest *FOM* of about 4200 $(\Omega\cdot cm)^{-1}$ (see Fig. 5.18). The difference of the *FOM* in this work and Lee et al. [37] is due to the difference in the deposition conditions such as RF power, argon gas pressure or the target used. We may conclude from Fig. 5.18 that the ZnO(Al) target with added Zn content of 1 wt % is suitable for preparing the ZnO(Al) thin films, better than that from the ZnO(Al) target with no Zn content added.

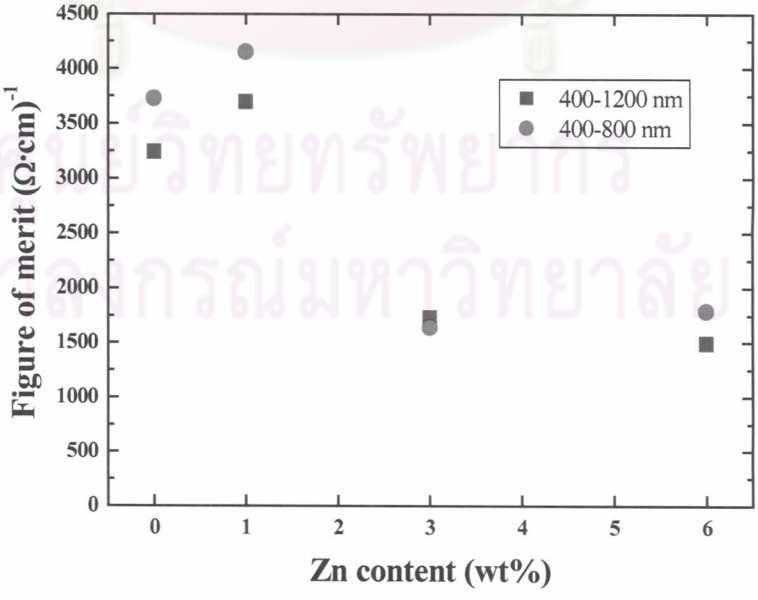

Figure 5.18: Variation of the figure of merit with the different ZnO(Al) targets.

The problem of the ZnO(Al) thin films prepared by the ZnO(Al) target with no Zn content added is that the films yield low resistivity and low transparency. Low transparency can cause the decreasing in the *FOM* and it is not suitable for making the window layer of solar cells. In this work, we prepared ZnO(Al) thin films by sputtering embedded–Zn ZnO(Al) targets and found that the target with added Zn content of 1 wt% yields the ZnO(Al) thin films with highest *FOM* due to the increase in the transparency. However, we note that the Zn content may vary from one method or machine to another.